

Hot corrosion of materials

Robert A. Rapp

Department of Materials Science and Engineering,
The Ohio State University,
Columbus, Ohio 43210 U.S.A.

Abstract - Alloys and ceramics may experience accelerated corrosion at high temperatures when their surfaces are coated by a thin film of fused salt in an oxidizing environment. Because of their high thermodynamic stabilities, fused alkali sulfates are frequently deposited or condensed onto hot substrates from the combustion product gases or else by the oxidation of heavy metal contaminants in the fuel, e.g. vanadium.

Solid-state electrochemical probes have been used in extensive determinations of the solubilities, and their dependencies on oxygen and Na_2O activities, for many important oxides in fused Na_2SO_4 at 1200K. The expectation for accelerated synergistic dissolution kinetics for two oxides of differing basicity has been confirmed experimentally.

Solid-state electrochemical probes have been attached at the surface of coupons of preoxidized nickel which were subjected to hot corrosion by a fused Na_2SO_4 film in an SO_2/O_2 gas environments. The probes were able to identify the onset of hot corrosion, and the local values for oxygen activity and the basicity in the salt film during the attack. The resulting data supported the Goebel-Pettit model for basic fluxing of nickel oxide and the negative solubility gradient criterion of Rapp-Goto.

The acidic solubilities of thermal barrier candidate oxides Y_2O_3 , CeO_2 and HfO_2 in a fused $0.7\text{Na}_2\text{SO}_4$ - 0.3NaVO_3 solution greatly exceed their solubilities in pure Na_2SO_4 , a problem which should exist for all oxides. A modeling of the constituent vanadates in the Na-V-S-O system permits a prediction of the dependence of oxide solubility on vanadium content and melt basicity.

INTRODUCTION

Many very important engineering systems operating at high temperatures (650-1100C) involve contact of metallic or ceramic materials with combustion product gases or other oxidizing gases containing inorganic impurities, e.g. gas turbines, steam generators, incinerators, and numerous petrochemical process vessels. As the gases are cooled, fused salt films may condense on the hardware to generate a highly corrosive condition analogous in some aspects to aqueous atmospheric corrosion. Some other engineering systems such as the carbonate fuel cell, heat treatment baths, etc., use high temperature salts to increase the kinetics of certain electrochemical and chemical reactions. Again materials come into contact with corrosive fused salt films which effect an accelerated degradation known as hot corrosion. The engineering application of high temperature systems, with their associated problems, is understood to be inherent in advanced technologies. As the availability of high quality fossil fuels becomes limited, and as the world seeks to incinerate solid wastes and to create more efficient energy conversion processes, etc., the occurrence and damage of hot corrosion is likely to increase.

A wealth of literature exists on the kinetics of hot corrosion, and on the resulting microstructures. Also, the chemistry and electrochemistry of hot corrosion have been reviewed rather recently (Ref. 1). In this paper, more recent developments in the chemistry and electrochemistry of hot corrosion are presented, and earlier papers presenting well known and accepted theories and experimental methods are referenced. Perhaps the three most important facts about the problem are these: 1. generally fused salts are electrolytic conductors so that the attack must be electrochemical in nature, 2. oxyanion fused salts (sulfates, carbonates, nitrates, etc.) exhibit an acid-base behavior that is crucial to most mechanistic aspects of hot corrosion, and 3. generally, metallic engineering alloys have virtually no regimes for mutual thermodynamic stability with a fused salt such as Na_2SO_4 , so that a corrosion product must form upon contact of the salt with the metallic substrate. Clearly, the avoidance of hot corrosion is achieved by forming a slow growing, compact and only slightly soluble oxide scale.

PHASE STABILITY

This subject has been treated in a manner exactly analogous to aqueous solutions by the formalism of Pourbaix, i.e. plots of electrode potential (oxidizing potential) vs. basicity, which for the pure Na_2SO_4 treated here, is defined as $-\log a_{\text{Na}_2\text{O}}$. The phase stability diagram for the Na-S-O system at 1200 K shown in Fig. 1 was derived from the standard Gibbs energies of formation for the compounds involved (Ref. 2). The broad stability field of Na_2SO_4 has been divided into regimes denoting the dominant minority ionic species, upon the assumption of an ideal solutions. This procedure is especially advantageous for the development of realistic interpretations for chemical and electrochemical reactions using the criterion that spontaneous reactions involve the consumption of unstable species and the formation of stable products for the local environmental conditions (coordinates of Fig.1). To measure accurately these conditions, a pair of solid-state tubular electrodes has been developed, forming a sodium-ion conducting electrolyte cell and an oxygen-ion conducting electrolyte cell, whose open-circuit potentials reveal the local oxidizing potential and the basicity according to well accepted expressions (Ref. 2). The emf's for these two reference electrodes in the regime of Na_2SO_4 stability have been indicated on Fig. 1.

With this understanding for the regime of stability for the electrolyte (or solvent) itself, one inquires about the phase stability for metals, oxides, or sulfides in contact with the fused salt. Figure 2 presents a phase stability diagram for the Ni-S-O system superimposed onto Fig. 1. Over a wide range of environmental conditions, the oxide NiO is stable in contact with fused Na_2SO_4 , although it exhibits a variable solubility as a basic solute NaNiO_2 and as the acidic solute NiSO_4 , as indicated by the dashed lines (-1, -2, -3) for the logarithm of the activities for these (fully ionized) species in fused Na_2SO_4 . Notably, there is only a negligible regime of conditions where the metal nickel could co-exist with fused Na_2SO_4 without reaction, usually to form a liquid nickel sulfide if an acid melt should contact the metal directly.

OXIDE SOLUBILITIES

The solubility of NiO in fused Ni_2SO_4 at 1200K and 1 atm O_2 pressure has been measured by atomic absorption analysis of NiO-saturated melts for well characterized basicities, as shown in Fig. 3 (Ref. 3). The dependencies of the acidic and basic solubilities on salt basicity (slopes in Fig. 3) agree exactly with those expected for constant activity coefficients for the dilute solutes. The calculated Henryan activity coefficients are 2.54 and 1.54 for the acidic and basic solutes, respectively. This illustrative example demonstrates the predictable solubility behavior for a simple oxide in a pure oxyanion solvent. According to the same methods, the solubilities of the oxides Al_2O_3 (Ref. 4), Co_3O_4 (Ref. 3), Cr_2O_3 (Ref. 5), iron oxides (Ref. 6), Y_2O_3 (Ref. 7),

SiO₂ (Ref. 8) and CeO₂ (Ref. 9) have been established in pure fused Na₂SO₄ at 1200K. Figure 4 presents a plot for the solubilities for most of these oxides at 1 atm oxygen. In every case, the dependencies for the acidic and basic solubilities on melt basicity are very well described by simple dissolution expressions analogous to those written in Fig. 3. Because of the valence changes for iron and chromium with changing oxygen activity, their solubilities have been shown to depend also on oxygen activity, again in a very predictable way. Because the oxide SiO₂ does not form any ionized acidic solute for the basicity range indicated in Fig. 4, the solubility of SiO₂ does not depend upon melt basicity. (However, in more basic melts, SiO₂ is subject to basic dissolution.)

HOT CORROSION MECHANISMS

This quantitative knowledge of these oxide solubilities represents an important background data bank for the interpretation of the mechanisms for Type 1 hot corrosion based on a scale fluxing/reprecipitation argument as first proposed by DeCrescente and Bornstein (Refs. 10, 11) and Goebel and Pettit (Ref. 12). Figure 5 presents a schematic diagram illustrating the

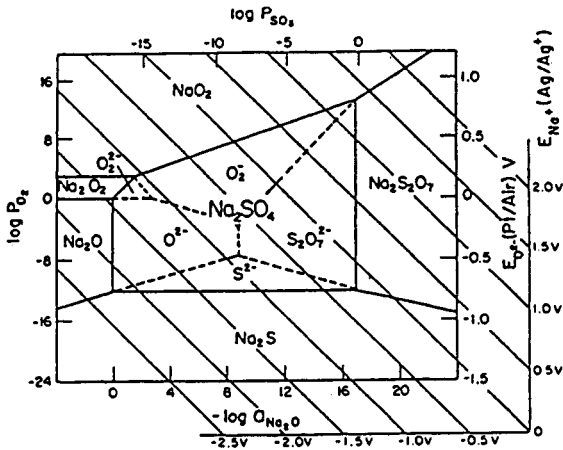


Figure 1: Phase stability diagram for Na-S-O System at 900C.

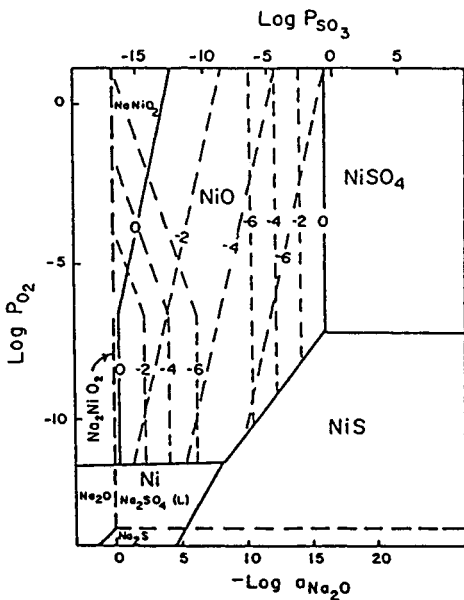


Figure 2: Na-Ni-S-O phase stability diagram for 1200K.

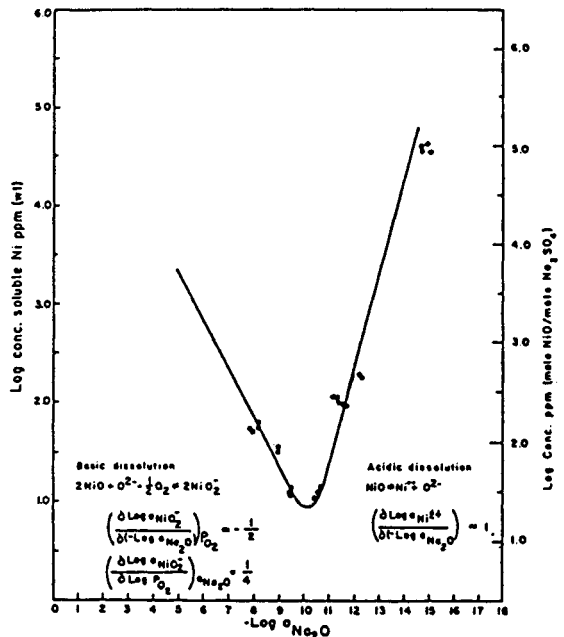


Figure 3: Solubility of NiO in fused Na₂SO₄ at 1200K.

fluxing of a protective scale on a pure metal and the precipitation of the same oxide as non-protective particles in the salt film. Rapp and Goto (Ref. 13) explained that the electrochemical nature of the hot corrosion process would lead to increased basicity at the site of the reduction reaction, so that basicity gradients, and associated solubility gradients, would be expected across the thin fused salt films. Accordingly, they suggested a negative solubility gradient for the protective oxide in the salt film as a criterion for a sustained hot corrosion attack. Goebel and Pettit (Ref. 12) had pointed out that contact between a nickel substrate and sodium sulfate would lead to sulfidation. Indeed, for the hot corrosion of nickel at high temperatures (Type 1), sulfides are found in the substrate, and oxide precipitates are formed within the salt film as schematized in Fig. 5.

Shores (Ref. 14) explained that the acidic dissolution of NiO cannot satisfy the "negative solubility gradient" criterion, and suggested that the salt film chemistry would be dominated by the acidic gaseous environment of

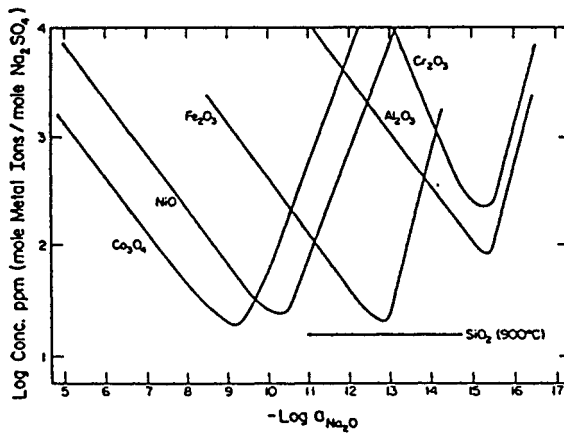


Figure 4: Experimentally established oxide solubilities in fused Na₂SO₄ at 1200K and 1 atm O₂.

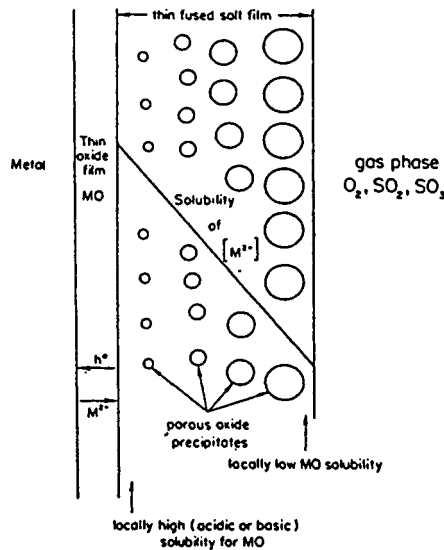


Figure 5: Dissolution-precipitation of MO oxide driven by a negative solubility gradient in a fused salt film.

gas turbine combustion products. Recently, Otsuka and Rapp (Ref. 15) used solid electrolyte probes attached to preoxidized nickel coupons which were then exposed to a thin film of Na_2SO_4 in an acid gas at 1173 K. The trace of the average local chemistry (coordinates for Fig. 1) for the salt film could then be followed as a function of time. As shown in Fig. 6, which plots the "reaction trace" as a function of time, a nickel coupon which suffered rapid, sustained hot corrosion actually was attacked by a basic salt to form a basic solute for NiO, to the left of the solubility minimum shown in Fig. 3. Indeed, the sulfidation of the Ni substrate greatly increased the basicity of the salt film, which was dominated by the interaction with the substrate and not the gas phase. This observation of basic hot corrosion of nickel was consistent with the views of several authors (Refs. 12-14). A different experiment whereby a preoxidized nickel coupon was exposed to a quite basic salt also resulted in rapid hot corrosion, although substrate sulfidation did not occur. In other experiments, Otsuka and Rapp (Ref. 15) were able to avoid hot corrosion by the formation of more protective initial NiO scales, and in that case, the local melt chemistry always remained to the right (acidic) side of the solubility minimum of Fig. 3. These studies established the validity for the "negative solubility gradient" criterion, which might, or might not, result from substrate sulfidation.

Another prediction from the paper by Rapp and Goto (Ref. 13) has been recently tested (Ref. 16). From an inspection of the widely spaced solubility curves of Fig. 4, and the model dissolution reactions written in Fig. 3, one would suppose that the simultaneous contact with fused sodium sulfate of two oxides with minima at differing basicity values could result in a synergistic accelerated dissolution of both the oxides. Namely, for an environment of basicity lying between the minima for two oxides, the oxide ions released upon the acidic dissolution of the more basic oxide would supply the reactant anions needed for the basic dissolution of the more acidic oxide. Hwang and Rapp (Ref. 16) measured the kinetics for the individual and the coupled dissolution for powders of Fe_2O_3 and Cr_2O_3 . In accord with prediction, as illustrated for Cr_2O_3 in Fig. 7, each of the oxides dissolved more rapidly in the presence of the second oxide for identical conditions otherwise. Synergistic dissolution could represent an impending danger for the usual sort of high-temperature alloys comprised of the basic base metals Fe, Ni, or Co in combination with the acidic protective components Cr or Al. If the initial stages of protective oxidation to develop Cr_2O_3 or Al_2O_3 scales would fail to exclude the presence of the transient oxides Fe_2O_3 , NiO, or CoO, then the two-phase scale should lead to the synergistic accelerated attack of both the acidic and the basic oxide, with the probable consequence of scale penetration by the salt and sulfidation of the substrate alloy.

The absence of any acidic ionic solute of silica, as indicated in Fig. 4, has led to a clear understanding for the excellent resistance to hot corrosion by fused Na_2SO_4 by the ceramics SiO_2 , and Si_3N_4 in acidic salts (Ref. 17). However, Jacobson found that the ceramics were rapidly attacked by the salt in the presence of (low acidity) air, as the silica formed the solute NaSiO_3 which was then reprecipitated in the salt film in accordance with a negative solubility gradient for SiO_2 . Basic sintering aids such as Y_2O_3 and MgO proved to assist in the attack of the ceramics by acidic fused Na_2SO_4 . Interestingly, both calculations and experiments showed that the combustion of lower quality fuel containing higher sulfur content was much less aggressive to the silica protective layer, since more acidic gaseous atmospheres were formed by combustion of high-sulfur fuel.

VANADATE CHEMISTRY AND OXIDE SOLUBILITIES

As high quality petroleum becomes more scarce and expensive, the use of fuel contaminated by heavy metals, especially vanadium, introduces a serious variation and complication to the hot corrosion of materials. Goebel et al. (Ref. 18) have shown that alloys containing Mo, W, or V, which oxidize to form the strongly acidic oxides MoO_3 , WO_3 and V_2O_5 , were

subject to an acidic dissolution attack of the protective oxides. Jones et al (Refs. 19,20) have studied the acid-base reactions between vanadate melts and various oxides to show qualitatively that the reactivity of Na-V-O melts is understood according to the following sequence of decreasing melt acidity: $V_2O_5 > NaVO_3 > Na_3VO_4$.

Zhang and Rapp (Ref. 9) measured the solubilities of the oxides CeO_2 , HfO_2 , and Y_2O_3 as a function of melt basicity at 1200K in a solvent of fused $0.7 Na_2SO_4 - 0.3 NaVO_3$ and the solubility of CeO_2 in pure Na_2SO_4 . The solubility plot for CeO_2 in the sulfate-vanadate solvent, shown in Fig. 8, obeys basicity dependencies for the basic and acidic solubilities which correspond exactly to the dissolution reactions:

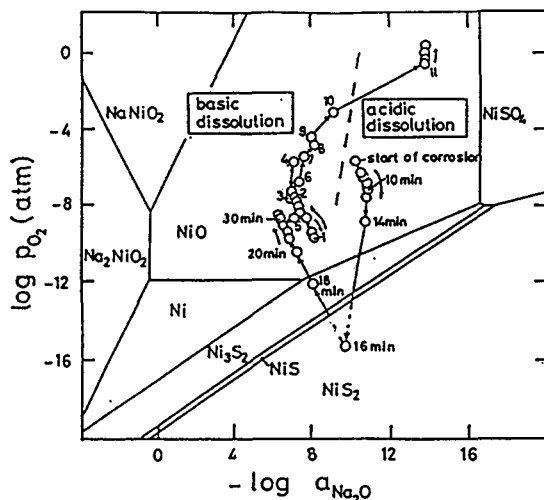
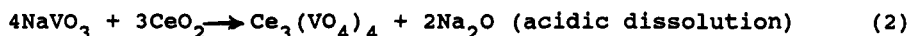


Figure 6: Trace of basicity and oxygen activity measured for preoxidized 99% Ni covered with a Na_2SO_4 film at 900C in $0.1\%SO_2-O_2$ gas atmosphere (preoxidized at 900C for 4 hours in O_2). Numbers designate reaction time in hours except as indicated severe corrosion.

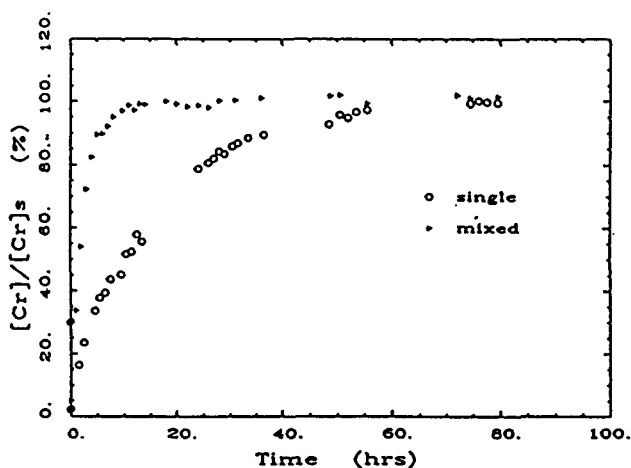


Figure 7: Time dependence of the normalized concentration of dissolved Cr_2O_3 (pure and mixed with Fe_2O_3) in fused Na_2SO_4 in $1\%SO_2-O_2$ gas at 1200K.

For the latter reaction, the final state may be envisioned as a dilute solution of Ce^{4+} ions dissolved in the mixed solution, whereby the complexing of O^{2-} ions by the reactant VO_3^- ions to form product VO_4^{3-} ions is the important driving force for the acidic dissolution. In fact, the solubility minimum for CeO_2 in the mixed solution occurred at surprisingly high values for both the basicity and for the magnitude of the minimum solubility. Similar results were found for the solubilities of HfO_2 and Y_2O_3 . Although, formally, the acidic solubility of CeO_2 can be described by the standard Gibbs formation energy and activity coefficient for the solute $\text{Ce}_3(\text{VO}_4)_4$, qualitatively the more important reaction involves the conversion of metavanadate ions to orthovanadate ions. For this reason Zhang and Rapp (Ref. 9) inferred that the acidic solubilities of most oxides would be affected similarly by the presence of metavanadate ions.

To establish the effect of 0.3NaVO_3 in Na_2SO_4 on the acidic dissolution of CeO_2 , the CeO_2 solubility was also measured in pure fused Na_2SO_4 at 1200K as a function of melt basicity. Figure 9 provides a comparison for the greatly different results. The solubility minimum for CeO_2 in pure Na_2SO_4 occurred in a much more acid melt, with a much lower magnitude for

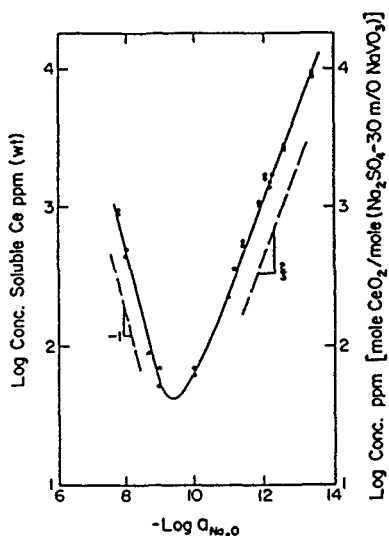


Figure 8: Solubility of CeO_2 in fused $0.7\text{Na}_2\text{SO}_4-0.3\text{NaVO}_3$ solution at 900C in 900C in 1 atm O_2 .

the minimum solubility. In other words, the 0.3NaVO_3 component of the mixed salt caused an important increase in the acidic solubility, and a similar effect must be expected for most oxides.

To extend, quantify, and generalize the stabilities of vanadates and their effect on the acidic solubilities of oxides, Hwang and Rapp (Ref. 21) assumed an ideal solution for the $0.7\text{Na}_2\text{SO}_4-0.3\text{VO}_{2.5}$ system to derive the equilibrium distribution of vanadate derivatives given in Fig. 10. In combination with the experimental use of the solid state electrochemical probes to measure the Na_2O activity, Fig. 10 permits a quantification of the stabilities for the vanadates, at least to the validity of the ideal solution assumption. By using the results of Fig. 9 and assuming a constant activity for the acidic solute of CeO_2 in $\text{Na}_2\text{SO}_4-\text{NaVO}_3$ solutions, the solubility of CeO_2 (or alternatively HfO_2 or Y_2O_3) can be calculated for other concentrations of NaVO_3 in fused Na_2SO_4 , as shown in Fig. 11. Only the line for 0.3NaVO_3 is a measured result;

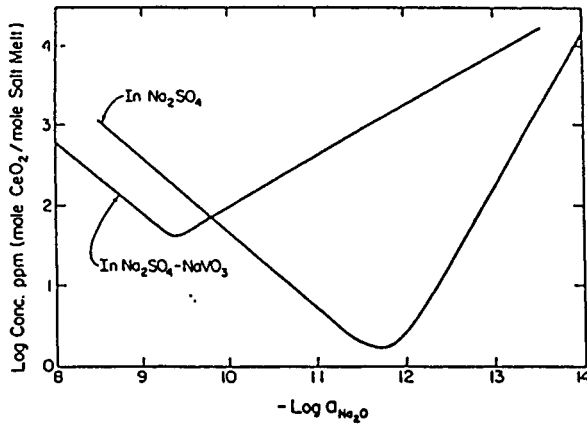


Figure 9: Comparison of solubilities for CeO_2 in pure fused Na_2SO_4 and in $0.7 Na_2SO_4-0.3NaVO_3$ at $900C$ in $1 atm O_2$.

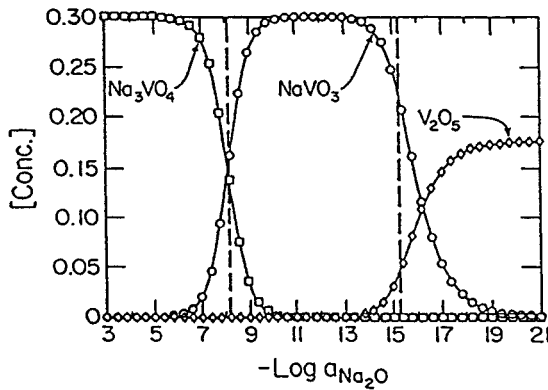


Figure 10: Equilibrium concentrations of Na_3VO_4 , $NaVO_3$, and V_2O_5 in $0.7Na_2SO_4-0.3NaVO_3$ in $1 atm O_2$ at $900C$.

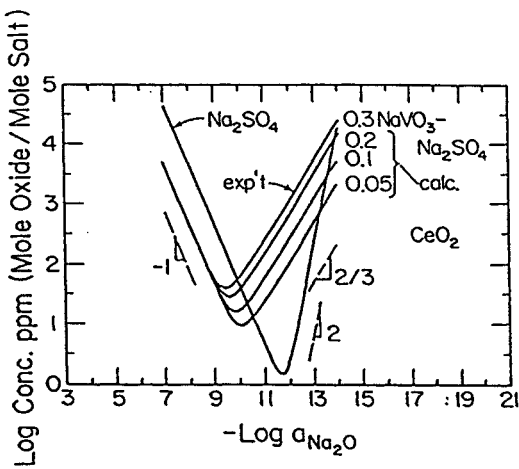


Figure 11: Solubilities of CeO_2 in $Na_2SO_4-xNaVO_3$ solutions at $900C$ in $1 atm O_2$ ($x = 0.3, 0.2, 0.1$ and 0.05).

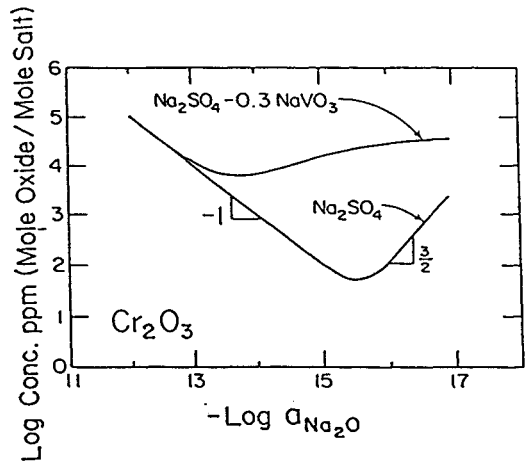


Figure 12: Measured solubility of Cr_2O_3 in pure Na_2SO_4 and calculated solubility for $0.7Na_2SO_4-0.3NaVO_3$ solution at $900C$ in $1 atm O_2$.

remarkably, even a low content of NaVO_3 in Na_2SO_4 results in an important increase in the acidic solubility of CeO_2 , or by generalization, of most other oxides. By the same procedure, by assuming that the known activity coefficient for the acidic solute for Al_2O_3 in pure Na_2SO_4 is retained in Na_2SO_4 - NaVO_3 melts, the solubility for Cr_2O_3 in the $0.7\text{Na}_2\text{SO}_4$ - 0.3NaVO_3 solution (where no experiments exist) can be estimated, as shown in Fig. 12. Obviously, such calculated behavior based on simplifying assumptions about the thermodynamic properties of the solutions requires experimental substantiation.

CONCLUSIONS

The solubilities of oxides and their dependencies of melt basicity and oxygen activity constitute important information to interpret hot corrosion mechanisms. Measurements of the local chemistry (reaction trace) in a thin fused Na_2SO_4 film during the hot corrosion of preoxidized Ni indicate a basic fluxing/reprecipitation of NiO according to a negative solubility gradient criterion for hot corrosion. The acidic solubilities of most oxides are raised by the presence of vanadate solutes in fused Na_2SO_4 . Calculations have been made, involving simple (reasonable) thermodynamic assumptions to interpret the thermochemistry of sodium sulfate-vanadate solutions and to predict the associated dependencies of oxide solubilities in these solutions.

Acknowledgement

This research was supported by the National Science Foundation, Metallurgy Programs of the Division of Materials Research, under Grant DMR 8620311.

REFERENCES

1. R.A. Rapp, Corrosion **42**, 568 (1986).
2. C.O. Park and R.A. Rapp, J. Electrochem. Soc. **133**, 1636 (1986).
3. D.K. Gupta, R.A. Rapp, J. Electrochem. Soc. **127**, 2194 and 2656 (1980).
4. P.D. Jose, D.K. Gupta, R.A. Rapp, J. Electrochem. Soc. **132**, 735 (1985).
5. Y.S. Zhang, J. Electrochem. Soc. **133**, 655 (1986).
6. Y.S. Zhang, R.A. Rapp, J. Electrochem. Soc. **132**, 734 and 2498, (1985).
7. M.L. Deanhardt, K.H. Stern, J. Electrochem. Soc. **129**, 2228 (1982).
8. D.Z. Shi, R.A. Rapp, J. Electrochem. Soc. **133**, 849 (1986).
9. Y.S. Zhang and R.A. Rapp, Corrosion **43**, 348 (1987).
10. N.S. Bornstein, M. A. DeCrescente, Trans. AIME **245**, 1947 (1969).
11. N.S. Bornstein, M.A. DeCrescente, Met. Trans. **2**, 2875 (1971).
12. J.A. Goebel, F.S. Pettit, Met. Trans. **1**, 1943 (1970).
13. R.A. Rapp, K.S. Goto, "The Hot Corrosion of Metals by Molten Salts, in Molten Salts", J. Braunstein, J.R. Selman, Eds., Electrochemical Society, Pennington, New Jersey, 81 (1981).
14. D.A. Shores, High Temperature Corrosion, NACE-6, R.A. Rapp, Ed., National Association of Corrosion Engineers, Houston, Texas, 493 (1983).
15. N. Otsuka and R.A. Rapp, "Local Salt Film Chemistry During Hot Corrosion of Preoxidized Nickel at 900C", to be published in Proceedings of TMS Symposium on High Temperature Corrosion, Feb. (1989).

16. Y.S. Hwang and R.A. Rapp, "Synergistic Dissolution of Oxides in Molten Salts", to be published in Proceedings of ASM/TMS Workshop on Oxidation of High-Temperature Materials, Oct. (1988).
17. N.S. Jacobson, Oxid. Metals **31**, 91 (1989).
18. J.A. Goebel, F.S. Pettit, G.W. Goward, Met. Trans. **4**, 261 (1973).
19. R.L. Jones, C.E. Williams, and S.R. Jones, J. Electrochem. Soc. **133**, 227 1986.
20. R.L. Jones and C.E. Williams, Surf. and Coatings Technol. **32**, 349 (1987).
21. Y.S. Hwang and R.A. Rapp, "Thermochemistry and Solubilities of Oxides in Sodium Sulfate-Vanadate Solutions", accepted for publication in Corrosion, March (1989).